Precise Shell Effects and Barriers from Fission Probabilities of Neighboring Isotopes

L. Phair, L. G. Moretto, K. X. Jing[1], L. Beaulieu[2], D. Breus,
J. B. Elliott, T. S. Fan[3], Th. Rubehn[4], and G. J. Wozniak

Nuclear Science Division, Lawrence Berkeley National Laboratory,
University of California, Berkeley, California 94720

Abstract. Fission excitation functions have been measured and analyzed for a chain of neighboring compound nuclei, from ^{207}Po to ^{212}Po. We present a new analysis which provides an accurate description of the fission barriers and ground state shell effects. Estimates of the fusion cross section are also obtained. The improved accuracy achieved in this analysis may lead to a future detailed exploration of the saddle mass surface.

The study of nuclei under extreme conditions (spin, isospin, temperature, and deformation) continues to be a major theme of nuclear physics. Fission is a fertile testing ground of nuclei under extreme deformation for several reasons.

A fissioning nucleus allows us to explore the *most* extreme nuclear deformation associated with a stationary point, well beyond that of super- or even hyper-deformation. Because the saddle configuration represents a bottleneck in phase space, a "stationary" point at which the probability to fission is determined, it is able to sustain its own spectroscopy. This spectroscopy manifests itself through the fission barrier, which can be thought of as a measurement of the mass of the saddle-point shape. This is seen immediately by considering the saddle mass (M_s) which is simply the ground state mass (M_{gs}) plus the experimental fission barrier (B_f) [1]. Consequently, the physics describing the saddle point mass surface should be similar to that of the ground state. For example, one should be able to explore the shape dependence of pairing, search for shell effects at the saddle, determine the shape dependence of the Congruence Energy (the Wigner term in the nuclear masses) [2] and the single particle level density at the saddle [3], etc.

Experimental fission barriers have also been disproportionately useful in fixing the adjustable parameters in theories of nuclear masses and deformabilities, and thus in the determination of basic properties of the nuclear fluid and its equation of state. The application of fission barrier measurements has also been important for the interpretation of many nuclear processes in which alpha, beta, proton and neutron emission compete with fission. The search for superheavy nuclei and the production of elements in astrophysical processes are examples.

Historically fission barriers have been measured anecdotally and with only moderate accuracy. The lack of precise and systematic data measured over a wide range of excitation energy has left the expectations mentioned in the introduction largely unfulfilled. In this work we provide new precision data, systematically measured for an isotopic chain of Po compound nuclei, covering a large excitation energy range. We also describe a new technique for analyzing this data which results in accurate fission barriers and ground state shell corrections.

The fission data were taken at the 88-Inch Cyclotron of the Lawrence Berkeley National Laboratory. We measured with high precision the fission excitation functions of the neighboring polonium compound nuclei ^{207,208,209,210,211,212}Po produced in ^{3}He- and ^{4}He-induced reactions on isotopically enriched lead targets (see Fig. 1).

We chose these particular reactions for several reasons. First, the shell corrections and fission barriers in the lead region are large and thus easier to measure. Second, the light ion induced reactions have only modest amounts of angular momentum ($< 25\hbar$). The relevant rotational energies are ≈ 2 MeV for a spherical shape and ≈ 0.8 MeV for the saddle shape of a Po nucleus with an angular momentum of $20\hbar$. And third, there are several stable isotopes of Pb from which one can make clean targets. The experimental details are described in ref. [4].

The solid and open symbols in Fig. 1 represent the fission cross section data for neighboring compound nuclei. The ^{4}He-induced reactions are shown in the left column and the ^{3}He-induced reactions are shown in the right. In two cases ($A = 211, 210$), we have overlap points where the same compound nucleus was formed via two different entrance

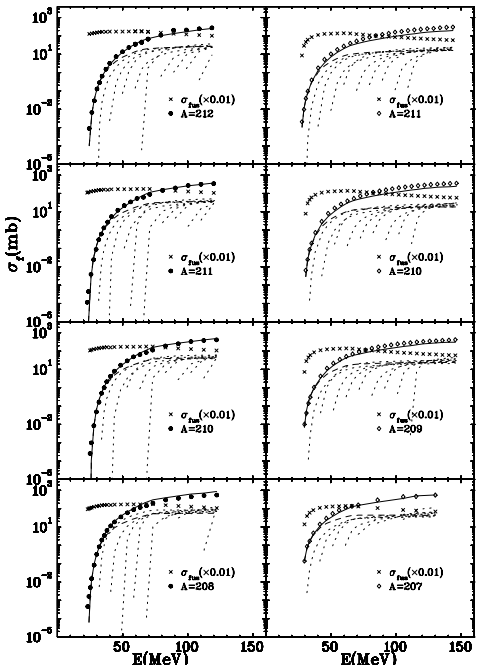

FIGURE 1. The fission cross section (symbols) is plotted as a function of excitation energy for the indicated compound nuclei. The dashed curve represents the first chance fission cross section. The dotted curves represent the second and higher chance fission cross sections. The solid curve is their sum, the total fission cross section. The left column contains α-induced reactions. The right contains ^{3}He-induced reactions.

channels.

To determine the fission probability, we use standard transition state theory as applied in ref. [4] and calculate the fission decay width

$$\Gamma_f = \frac{1}{2\pi\rho(E)} \int \rho_s(E - B_f - \varepsilon) d\varepsilon. \tag{1}$$

where ρ_s is the level density at the saddle, ε is the kinetic energy associated with the fission channel, and ρ is the level density of the compound nucleus.

The width for neutron emission (the only other exit channel assumed in our analysis) is given by

$$\Gamma_n = \frac{2mR^2 g\prime}{\hbar^2} \frac{1}{2\pi\rho(E)} \int \varepsilon \rho_d(E - B_n - \varepsilon) d\varepsilon. \tag{2}$$

where m denotes the neutron mass, R is the radius and ρ_d is the level density of the daughter nucleus after neutron emission, $g\prime$ is the spin factor (2), B_n is the neutron binding energy, and ε is the kinetic energy of the neutron.

Expanding the log of the level density in the integral and taking into account the angular momentum a fissioning nucleus may have, Eqs. (1) and (2) can be evaluated and their ratio taken so that Γ_f/Γ_n

$$\frac{\Gamma_f}{\Gamma_n} = \frac{T_s - \frac{1}{2a_f}}{K\left(T_n^2 - \frac{3}{2a_d}T_n + \frac{3}{4a_d^2}\right)} \frac{\rho_s(E - B_f - E_r^s)}{\rho(E - B_n - E_r^{gs})} \tag{3}$$

where a_f and T_s denote the level density parameter and temperature at the saddle, a_d and T_n denote the level density parameter and temperature of the residual daughter after neutron emission, and E_r^s and E_r^{gs} denote the rotational energy of the system at the saddle point and the energy of the rotating ground state. As mentioned previously, the rotational energies are small because of the very asymmetric entrance channels. The ground state and saddle moments of inertia were taken from Sierk [5].

For nuclei with strong shell effects, the approximation $\rho(E - B_n - E_r^{gs}) \propto \exp(2\sqrt{a_d(E - B_n - E_r^{gs})})$ becomes a poor one. The shell effects of a nucleus affect its level density in a rather complicated way at low energies. But at

high enough excitation energies, we can use the asymptotic form $\rho(E) \propto \exp(2\sqrt{a(E+\Delta_{\rm shell})})$ [6]. For the daughter nucleus produced by neutron emission, the level density takes the asymptotic form:

$$\rho_d(E - B_n - E_r^{gs}) \propto \exp\left(2\sqrt{a_d(E - B_n - E_r^{gs} + \Delta_{\rm shell}^{n-1})}\right) \tag{4}$$

where $\Delta_{\rm shell}^{n-1}$ is the ground state shell effect of the daughter nucleus after neutron emission.

For the level density at the saddle point (ρ_s), the problems should be far less serious. On the one hand, the large deformations at the saddle point imply small shell effects there. On the other hand, there is a topographic theorem which states that the saddle masses should be close to those calculated using a macroscopic theory without shell effect corrections at the saddle [7]. However, if this assumption is incorrect, the extracted fit parameters will reflect this.

Pairing effects also affect the level density in a manner similar to that of the shell effects. The level density is evaluated at an energy shifted by the condensation energy ΔE_c. The condensation energies are calculated separately for protons and neutrons. For an even-even nucleus, $\Delta E_c = \frac{1}{2} g_n \Delta_n^2 + \frac{1}{2} g_p \Delta_p^2$ where $g_n = (3/\pi^2) a_n$, $g_p = (3/\pi^2) a_p$, and $a_d = a_n + a_p = N/8.5\ \mathrm{MeV}^{-1} + Z/8.5\ \mathrm{MeV}^{-1} = A/8.5\ \mathrm{MeV}^{-1}$. For an even-odd nucleus $\Delta E_c = \frac{1}{2} g_n \Delta_n^2 + \frac{1}{2} g_p \Delta_p^2 - \Delta_n$, and in general

$$\Delta E_c = \frac{1}{2} g_n \Delta_n^2 + \frac{1}{2} g_p \Delta_p^2 - \mathrm{mod}(N,2)\Delta_n - \mathrm{mod}(Z,2)\Delta_p. \tag{5}$$

The ground state gap parameters for protons (Δ_p) and for neutrons (Δ_n) were chosen to be

$$\Delta_p = \Delta_n = \frac{12\mathrm{MeV}}{\sqrt{A}}. \tag{6}$$

At the saddle, the gap parameter for the neutrons(Δ_n^f) was taken to be $\Delta_n^f = S e^{-\frac{1}{g_n^f G}}$ where S and G were chosen to reproduce the ground state values (Eq. (6)) and $g_n^f = (3/\pi^2)(N/A) a_f$. A similar expression for Δ_p^f can be calculated for protons using $g_p^f = (3/\pi^2)(Z/A) a_f$. Consequently, we express the condensation energy at the saddle as

$$\Delta E_c^s = \frac{1}{2} g_n^f (\Delta_n^f)^2 + \frac{1}{2} g_p^f (\Delta_p^f)^2 - \mathrm{mod}(N,2)\Delta_n^f - \mathrm{mod}(Z,2)\Delta_p^f \tag{7}$$

The resulting expression for Γ_f/Γ_n is

$$\frac{\Gamma_f}{\Gamma_n} \propto e^{2\sqrt{a_f\left(E - B_f - E_r^s - \Delta E_c^f\right)} - 2\sqrt{a_d\left(E - B_n - E_r^{gs} + \Delta_{\rm shell}^{n-1} - \Delta E_c\right)}}. \tag{8}$$

We further assume that the fission barrier can be broken into two parts

$$B_f = B_{\rm macro} - \Delta_{\rm shell} \tag{9}$$

where for the macroscopic part ($B_{\rm macro}$) we take a scaled value of the Thomas-Fermi predictions [1], and the microscopic part is the ground state shell correction for this nucleus.

The expression for Γ_f/Γ_n (Eq. (8)) has four free parameters: $B_{\rm macro}$, $\Delta_{\rm shell}$ of the fissioning system, $\Delta_{\rm shell}^{n-1}$ of the 1 neutron-out daughter nucleus, and the ratio of the level density parameters a_f/a_d.

To make use of this description of Γ_f/Γ_n, we write the total fission cross section as

$$\sigma_f = \sum_{i=0} \sigma_f^{(i)} = \sum_{l=0}^{l=l_{\rm max}} \sum_{i=0} \sigma_l P_f^{(i)}(l) \tag{10}$$

where $\sigma_f^{(i)}$ is the fission cross section after i neutrons have been emitted, σ_l is the angular momentum distribution of the fusion cross section ($(2l+1)\pi\bar{\lambda}^2$), $l_{\rm max}$ comes from the assumed fusion cross sections (crosses in Fig. 1) and $P_f^{(i)}(l)$ is the fission probability after the emission of i neutrons from a compound nucleus of initial angular momentum l. The fission probability at each "step" i and initial angular momentum l can be written as

$$P_f^{(i)}(l) = \frac{1}{1 + \frac{\Gamma_n}{\Gamma_f}(l,i)} \tag{11}$$

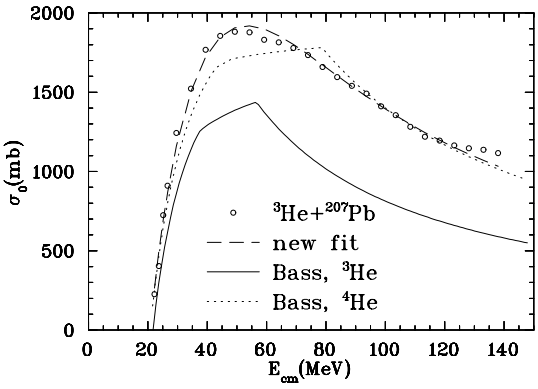

FIGURE 2. The fusion cross section (open circles) as described in the text extracted for the reaction ^{3}He+^{207}Pb is plotted as a function of the center of mass energy. The Bass model prediction [8] is given by the solid line. The Bass model prediction for the ^{4}He-induced reaction is given by the dotted line. The empirical fit of Eq. (12) is given by the dashed line.

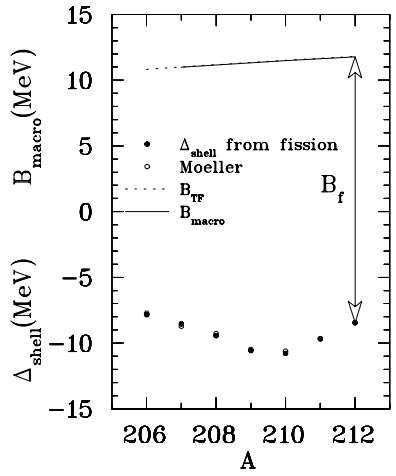

FIGURE 3. The shell corrections extracted from the fission fits (solid circles) are plotted as a function of mass number. The open circles represent the ground state shell correction estimated by Möller *et al.* [9]. The solid line is the macroscopic barrier extracted from the fission fit and the dashed line is a Thomas-Fermi estimate [1]. The difference between the the macroscopic barrier $B_{\rm macro}$ and the shell correction $\Delta_{\rm shell}$ is the fission barrier B_f.

where the angular momentum dependence comes in through the rotational energy dependence of Γ_f/Γ_n and the "multiple-chance" energy dependence is accounted for on average by assuming that with the emission of each neutron, the excitation energy drops by $2T + B_n$.

With Eqs. (3), and (8)-(11), we are prepared to fit the fission data for a chain of neighboring isotopes.

However, a remark regarding the fusion cross sections is in order at this point. If we use the Bass model description of the fusion cross sections and fit the fission cross sections with the method outlined above, we get reasonable fits to the α-induced reactions, but somewhat poorer fits for the ^{3}He-induced reactions. Since we have fission measurements for the same compound nucleus (e.g. ^{210}Po) produced with two different entrance channels, we can estimate the fusion cross section for one of the channels. We have fit all the α-induced reactions and fixed the resulting fission parameters. We then fit the ^{3}He-induced reaction on ^{207}Pb and varied only the fusion cross sections to obtain a perfect fit. The resulting fusion cross sections are shown by the open circles in Fig. 2. The Bass model prediction (solid line) underpredicts this estimate by nearly a factor of two at the highest energies, but it has the correct overall shape. In fact the Bass model prediction for the α-induced reactions (dotted line) gives reasonably good agreement.

We have chosen to fit the fusion cross section with the following form:

$$\sigma_0 = \frac{b}{E_{cm}} \pi R^2 \tanh\left(\frac{E_{cm} - V}{b}\right) \tag{12}$$

where V represents the fusion barrier, πR^2 is a geometric cross section and b determines the high energy behavior of σ_0. Note that in the low energy limit ($E_{cm} \approx V$), Eq. (12) goes to $\sigma_0 = \pi R^2(1 - V/E_{cm})$ and at high energies σ_0 goes to $\sigma_0 = bE_{cm}\pi R^2$. The resulting fit is given by the dashed line in Fig. 2. It is this fit that we have used for all of the fusion cross sections in this report.

With this choice of fusion cross sections we are ready to proceed and fit the fission cross sections. Note that this new fitting technique requires a self-consistent global description of the data. For example, the third chance fission for nucleus A uses the same fission barrier as the second chance fission of nucleus $A-1$, which is the same barrier as first chance fission of nucleus $A-2$. This global description of the fission cross sections produces remarkable results.

The total fission cross sections calculated using Eq. (10) are shown as the solid lines in Fig. 1. The dashed line represents "first-chance" fission. The dotted lines represent second, third and higher chance fission yields.

To fit all of the systems in Fig. 1, nine free parameters were taken: one to describe the A dependence of the macroscopic barriers, two to describe the smooth (assumed linear) dependence of the ratio a_f/a_d as a function of A, and one each to describe shell correction for the 1n daughter channel for each of the fissioning systems (the shell correction for ^{212}Po was fixed at the Möller value [9]).

The extracted Δ_{shell} values are shown by the solid circles in Fig. 3. The values of Δ_{shell} show a clear shell closure at $A = 210$ ($N = 126$). Furthermore, there is a remarkable agreement between the values from the present fission analysis and those determined by Möller *et al.* in fitting the ground state masses [9] (open circles). The mean deviations are smaller than 200 keV. The agreement is remarkable, especially when compared to earlier attempts [10]. In the early attempts, the fission cross sections were fit for a single system (one compound nucleus using a first chance only formalism) and the uncertainties were typically ± 1.5 MeV. The present analysis represents a vast improvement.

The extracted fission barriers are shown in Fig. 3 as a difference between the shell correction and the macroscopic barriers. The macroscopic barrier from the fit is given by the solid line and is nearly indistinguishable from the Thomas-Fermi prediction (solid line) [1]. With data at other fissilities, it should be possible to explore systematic changes in the macroscopic barriers, in particular the predicted shape changes of the congruence energy [2].

The ratio a_f/a_d has an average value of ≈ 1.01 with a slight dependence on A. With additional data at other values of fissility, it should be possible to study the surface area (or fissility) dependence of a_f [3].

In summary, we have reported new precision fission data, and we have demonstrated the extraction of accurate fission barriers and ground state shell corrections with a new method of globally fitting fission data for an isotopic chain of nuclei. An accurate description of the saddle mass configuration may open avenues that have been explored extensively for ground state masses. For example, it may soon be possible to address pairing corrections at the saddle, the surface area (or fissility) dependence of both the saddle level density and the macroscopic barrier, and even shell effects at the saddle in a quantitative fashion. As more data becomes available, especially at the new radioactive beam facilities, the techniques presented here may prove valuable for an accurate description and understanding of the fission "saddle-mass" surface.

Present addresses:
[1] Physics Dept., Sichuan Univ., Chengdu, China
[2] beaulieu@phy.ulaval.ca
[3] Tech. Physics Dept., Peking Univ., Beijing, China
[4] Rubehn@t-online.de

REFERENCES

1. W.D. Myers and W.J. Swiatecki, Phys. Rev. C **60**, 4606 (1999).
2. W.D. Myers and W.J. Swiatecki, Nucl. Phys. A **612**, 249 (1997).
3. J. Toke and W.J. Swiatecki, Nucl. Phys. A **372**, 141 (1981).
4. Th. Rubehn, *et al.*, Phys. Rev. C **54**, 3062 (1996).
5. Sierk, private communication.
6. J. R. Huizenga and L. G. Moretto, Ann. Rev. Nucl. Phys. **22**, 427 (1972).
7. W.D. Myers and W.J. Swiatecki, Nucl. Phys. A **601**, 141 (1996).
8. R. Bass, Phys. Rev. Lett. **39**, 265 (1977); Nucl. Phys. A **231**, 45 (1974).
9. P. Möller, *et al.*, At. Data Nucl. Data Tab. **59**, 185 (1995).
10. L.G. Moretto, *et al.*, Phys. Rev. Lett. **75**, 4186 (1995).